Characterization of Novel *O*-Glycans Isolated from Tear and Saliva of Ocular Rosacea Patients

Sureyya Ozcan,[†] Hyun Joo An,[‡] Ana C. Vieira,[§,||] Gun Wook Park,[‡] Jae Han Kim,[⊥] Mark J. Mannis,[§] and Carlito B. Lebrilla*[†,#]

[†]Department of Chemistry and [#]Department of Biochemistry and Molecular Medicine, University of California, Davis, Davis, California 95616, United States

[‡]Graduate School of Analytical Science and Technology and [⊥]Department of Food Nutrition, Chungnam National University, Daejeon, Korea 305-764

[§]Department of Ophthalmology & Vision Science, University of California, Davis Health System Eye Center, Sacramento, California 95817, United States

[||]Department of Ophthalmology, Federal University of São Paulo, São Paulo, Brazil

ⓢ *Supporting Information*

ABSTRACT: *O*-Glycans in saliva and tear isolated from patients suffering from ocular rosacea, a form of inflammatory ocular surface disease, were profiled, and their structures were elucidated using high resolution mass spectrometry. We have previously shown that certain structures, particularly sulfated oligosaccharides, increased in the tear and saliva of rosacea patients. In this study, the structures of these glycans were elucidated using primarily tandem mass spectrometry. There were important similarities in the glycan profiles of tears and saliva with the majority of the structures in common. The structures of the most abundant species common to both tear and saliva, which were also the most abundant species in both, were elucidated. For sulfated species, the positions of the sulfate groups were localized. The majority of the structures were new, with the sulfated glycans comprising mucin *core 1*- and *core 2*-

type structures. As both saliva and tear are rich in mucins, it is suggested that the *O*-glycans are mainly components of mucins. The study further illustrates the strong correspondence between the glycans in the tear and saliva of ocular rosacea patients.

KEYWORDS: *O*-glycan, saliva, tear, mass spectrometry, structural characterization, sulfated *O*-glycan, sialylated *O*-glycan
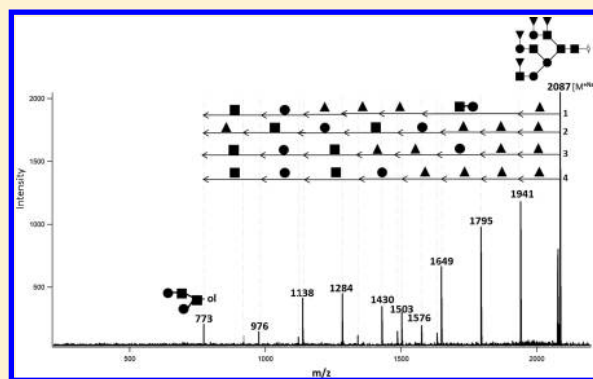
■ INTRODUCTION

Glycomics, the comprehensive study of glycans expressed in a biological system, has recently emerged as a promising area for disease marker discovery.[1−7] Glycosylation mediates a number of essential biological functions including cell−cell and cell−-matrix recognition, cellular adhesion, and inter- and intracellular interaction.[4,7,8] It is also one of the most common forms of post-translational modifications.[9] Two main forms of glycosylation occur in eukaryotes: *N*-glycosylation, in which a glycan moiety is attached to an asparagine (Asn) residue, and *O*-glycosylation, in which a glycan moiety is attached to either a serine (Ser) or threonine (Thr) residue.[10−14]

Human tear and saliva are biological fluids that are readily accessible and may act as a mirror of health status. Saliva is a complex and versatile body fluid that supplies a wide range of physiological needs. It is secreted by salivary glands (parotid, submandibular, and sublingual) and is composed of a complex mixture of mucin, amylase, lingual lipase, electrolyte solutions, proteins, and enzymes.[15,16] Tear includes a complex mixture of proteins including mucin and electrolytes. Interestingly, mucins

are one of the primary components in both saliva and tears. Mucins are biopolymers consisting of very long polypeptide chains that are highly *O*-glycosylated with heterogeneous collections of structures. From this perspective, they are a remarkable source of material for glycomics analysis. Recent studies show that several diseases are associated with aberrant glycosylation in mucins.[17−25]

The glycomes of tear and saliva have not been well characterized possibly due to the complexity of the glycosylation and limitations in analytical tools.[19,26,27] Mucins are remarkably heavily glycosylated proteins, consisting of as much as 50−80% carbohydrates by mass. As a result, mucin-type *O*-glycosylated proteins are usually greater than 200 kDa, with the *O*-glycan attached to the protein in deny clusters. *O*-Glycosylated mucins generally interface between epithelial cells and the external environment.[26,28] Mucins impact the biological processes of many diseases. For instance, recent studies indicate that many

transmembrane mucins are aberrantly overexpressed in various cancers[29] as well as cystic fibrosis.[30] *O*-Glycosylation has no known consensus sequence and may potentially be found at any serine or threonine residue in mucin. *O*-Glycans are built on eight possible core structures, with *core 1* and *core 2* being the most common.[26,31,32]

Sulfated glycans make up mucin glycosylation along the respiratory and gastrointestinal tracts. They are also found in salivary glands. Sulfated oligosaccharides are involved in chemical defense, hormone biosynthesis, and bio activation. For example, *Helicobacter pylori* can bind avidly to sulfated glycans on high molecular weight salivary mucins.[33−35] Generally, sulfate-containing glycans protect against the toxic or potentially toxic effects of numerous xenobiotics and their metabolites. Sulfated glycoconjugates are polar and are highly water-soluble, making them more readily excreted in urine or bile. They may exhibit reduced pharmacological/biological activity with respect to the parent compound.[31,36]

Rosacea is a common and chronic cutaneous disorder. It is characterized by inflammation that is primarily localized on central face where the cheek, nose, chin, forehead, and eyelid become red. Ocular rosacea is a specific subtype of rosacea. The diagnosis of ocular rosacea is remarkably challenging especially for the patients that do not present with typical skin findings but have ocular signs and symptoms such as dry eye and a characteristic form of blepharitis. At the present time, there is currently no objective diagnostic method for ocular rosacea.[37−39] The frequent presence of dry eye in patients with rosacea can make clinical studies difficult due to the paucity of tear samples. Hence, other biological fluids such as saliva may be used as an alternative to tears.[40]

An earlier study from this group demonstrated significant differences between control and rosacea patients in the *O*-glycan profiles of tear fluids.[19] We found that sulfated oligosaccharides released from mucins in tears were highly up-regulated in ocular rosacea patients. However, basal tear samples from individuals are limited, and there were insufficient amounts to confirm glycan compositions or structures. Instead, accurate mass was used to determine the glycan compositions, but the presence and the positions of the sulfated groups could not be confirmed by tandem mass spectrometry (MS).

In the present study, we confirm the presence of sulfated glycans in the tear fluid of rosacea patients. Furthermore, because the tear and saliva are distinct but physiologically connected fluids, it was decided that the inclusion of saliva in this study would provide additional and possibly novel insights into the ocular disease. This study demonstrates that glycan structures in tears and saliva are related and correlate in disease states. The rapid and sensitive characterization of novel glycans found in these fluids offers a promising new method for the diagnosis of ocular rosacea and other related diseases.

■ MATERIALS AND METHODS

Sampling

Tear fluid and saliva samples were collected from patients with ocular rosacea and the control group. Tear fluid samples (23 patients with ocular rosacea and 28 controls) were collected from the inferior tear meniscus by using 10 μL microcapillary tubes (Microcaps, Drummond Scientific Co, Broomall, PA). Saliva samples (17 patients and 25 controls) from the same subjects were obtained with the aid of disposable plastic pipettes from sublingual glands. The subjects were required to avoid eating,

drinking, or the use of oral hygiene products for at least 1 h prior to saliva collection. The patients were also required to cease the use of any eye drops 1 h prior to tear collection. All samples were frozen at −80 °C until analysis.

Chemical Release of *O*-Glycans from Tear Fluid and Saliva by *β*-Elimination

O-Glycans were directly released from human fluids without protein identification. There is currently no general enzyme for *O*-glycan release. Thus, samples were directly released by *β*-elimination. Saliva and tear samples were pooled in the range of 8−15 samples depending on how much sample was available. Five microliters of saliva and tear from each subject was pooled to obtain a homogeneous representative sample. Twenty microliters of the pooled sample and 20 μL of alkaline borohydride solution (mixture of 1.0 M sodium borohydride and 0.1 M sodium hydroxide) were mixed. The mixture was incubated at 42 °C for 16 h in a water bath. The reaction was stopped by adding 1.0 M hydrochloric acid solution until pH of the solution reached pH 5. During this procedure samples were kept in an ice bath.[19]

Glycan Purification and Fractionation

The chemically released oligosaccharides were purified and fractionated by a porous graphitized carbon (PGC) cartridge to minimize suppression of glycans. The GC cartridge was washed with an aqueous solution of 80% (v/v) acetonitrile and 0.01% (v/v) trifluoroacetic acid (6 mL total) at a flow rate of about 3 mL/min. The cartridge was equilibrated by adding 6 mL of nanopure water at a flow rate of 3 mL/min. Tear fluid and saliva samples were loaded onto the PGC cartridge by gravity. Subsequently, the cartridge was washed by gravity with nanopure water (12 mL total) at a flow rate of 1 mL/min. The glycans were eluted by 6 mL of 20% acetonitrile in water and 6 mL of 40% acetonitrile in water with 0.05% (v/v) trifluoroacetic acid solutions according to their polarities. Each fraction was evaporated to dryness and reconstituted by adding 15 μL of nanopure water prior to matrix-assisted laser desorption/ionization mass spectrometry (MALDI-MS) and liquid chromatography (LC) chip quadrupole-time-of-flight (Q-TOF) analyses.

Mass Spectrometric Analysis by MALDI-FTICR-MS

Glycan profiling was monitored by using MALDI-FTICR-MS. Mass spectra were recorded on an external source HiResMALDI (IonSpec, Irvine, CA, USA) equipped with a 7-T magnet. The instrument was equipped with a pulsed Nd:YAG (neodymium-doped yttrium aluminum garnet; $Nd:Y_3Al_5O_{12}$) laser (355 nm). 2,5-Dihydroxybenzoic acid was used as a matrix (50 mg/mL in 50% acetonitrile (AcN)). A saturated solution of NaCl in was used as a cation dopant.

Mass Spectrometric Separation by LC Chip Q-TOF MS

Fractionated and enriched glycans were analyzed by using an Agilent 1200 series LC system connected to an Agilent 6520 Q-TOF MS (Agilent Technologies, Santa Clara, CA). The nanoLC-Chip/Q-TOF system was equipped with a micro well-plate auto sampler (maintained at 6 °C), a capillary loading pump for sample enrichment, a nanoflow pump as the analytical pump for sample separation, a nano LC-Chip Cube, and the Agilent 6520 Q-TOF MS detector. Data dependent tandem MS were obtained following LC separation on the microfluidic chip consisting of a 4 mm × 0.040 mm i.d. enrichment column and a 43 mm × 0.075 mm i.d. analytical column, both packed with 5 μm porous graphitized carbon (PGC) as a stationary phase. LC separation was obtained by using binary gradient solvent A, 3.0% acetonitrile/water (v/v) with 0.1% formic acid and B, 90%
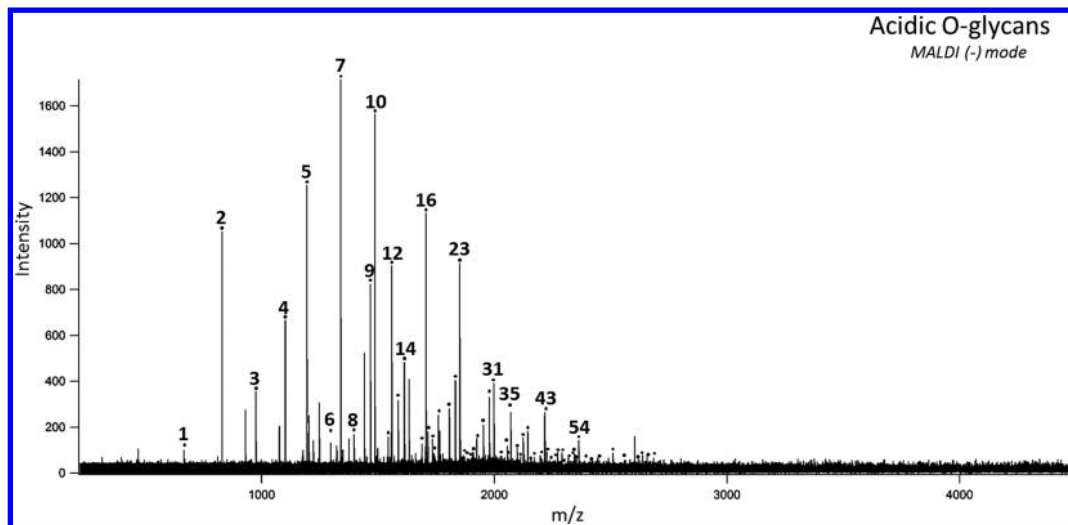
Figure 1. Representative MALDI FT-ICR mass spectrum of *O*-glycans released from tear of a patient with ocular rosacea in negative mode. The signals correspond primarily to sulfated oligosaccharides. The label numbers correspond to specific glycan compositions listed in Table 1.

Table 1. Acidic *O*-Glycans Found in Diseased Tear As Observed by Negative Mode MALDI FT-ICR MS[a]

peak ID	[M − H]⁻	H	F	N	SA	s	peak ID	[M − H]⁻	H	F	N	SA	s
1	667.191	1		2		1	32	2012.619	2		6	1	2
2	829.241	2		2		1	33	2045.625	4		6		2
3	975.283	2	1	2		1	34	2054.700	4	2	5		1
4	1178.379	2	1	3		1	35	2070.695	5	1	5		1
5	1194.374	3		3		1	36	2086.687	6		5		1
6	1324.437	2	2	3		1	37	2095.727	3	2	6		1
7	1340.431	3	1	3		1	38	2101.645	2	2	5	1	2
8	1397.459	3		4		1	39	2126.737	3	3	4	1	1
9	1470.498	2	3	3		1	40	2141.744	7		2	2	
10	1486.484	3	2	3		1	41	2183.749	3	2	5	1	1
11	1543.506	3	1	4		1	42	2200.758	4	3	5		1
12	1559.512	4		4		1	43	2216.753	5	2	5		1
13	1615.545	2	2	3	1	1	44	2241.782	3	3	6		1
14	1632.556	3	3	3		1	45	2257.788	4	2	6		1
15	1689.559	3	2	4		1	46	2273.790	5	1	6		1
16	1705.557	4	1	4		1	47	2289.798	4	5	4		1
17	1714.632	1	3	5		1	48	2305.790	5	4	4		1
18	1730.588	2	2	5		1	49	2321.742	3	3	6		2
19	1746.594	3	1	5		1	50	2329.837	6	3	3	1	
20	1762.592	4		5		1	51	2346.824	4	4	5		1
21	1794.597	4	3	3		1	52	2362.811	5	3	5		1
22	1835.624	3	3	4		1	53	2371.849	2	5	6		1
23	1851.611	4	2	4		1	54	2403.844	4	3	6		1
24	1867.625	5	1	4		1	55	2435.829	6	1	6		1
25	1892.656	3	2	5		1	56	2449.765	2	1	6	2	2
26	1908.647	4	1	5		1	57	2465.759	3		6	2	2
27	1924.660	3	5	3		1	58	2549.899	4	4	6		1
28	1938.609	4		3	2	1	59	2611.821	3	1	6	2	2
29	1965.658	4		6		1	60	2622.918	5	2	7		1
30	1980.672	3	2	4	1	1	61	2636.935	7	2	3	2	
31	1997.677	4	3	4		1							

[a]H = hexose, F = fucose, N = *N*-acetylhexosamine, SA = sialic acid, s = sulfate group.

acetonitrile/water (v/v) with 0.1% formic acid. A flow rate of 4 μL/min of solvent A was used for sample loading with a 2 μL injection volume. Gradient separation was performed using 0% B (0.00−2.50 min), 0 to 16% B (2.50−20.00 min), 16% to 44% B (20.00−30.00 min), 44% to 100% B (30.00−35.00 min), and 100% B (35.00−45.00 min). The drying gas temperature was set to 325 °C with a flow rate of 4 L/min. MS and MS/MS spectra were obtained in the positive ionization mode with an acquisition time of 1587 ms per spectrum and acquisition rate of 0.63 spectra per second. Tandem MS obtained by collision induced fragmentation with nitrogen as the collision gas using a series of collision energies that were dependent on the *m/z* values of

the different glycans. The collision energies correspond to voltages ($V_{collision}$) that were based on the equation $V_{collision} = m/z$ (1.8/100 Da) V − 2.4 V, where the slope and offset of the voltages were set at (1.8/100 Da) and (−2.4), respectively.

■ RESULTS AND DISCUSSION

Sulfated glycans were shown to increase in ocular rosacea.[40] However, in the previous study limited amounts of sample made

Table 2. Low Abundance _O_-Glycans in Diseased Tear Obtained by Positive Mode Nano LC CHIP Q-TOF MS[a]

peak ID	[M]	H	F	N	SA	s
1	426.185			2		
2	465.138	1		1		
3	514.199			1	1	
4	531.210	1	1	1		
5	676.253	1		1	1	
6	750.290	2		2		
7	756.233	1		1	1	1
8	880.354	1	2	2		
9	910.250	2		2	2	
10	967.349	1	2	1		
11	1042.406	2	2	2		
12	1066.417		1	3	1	
13	1201.346			2	2	1
14	1412.461	2	2	2		1
15	1558.519	2	1	2	2	1

[a]H = hexose, F = fucose, N = N-acetylhexosamine, SA = sialic acid, s = sulfate group.

structural analysis of the sulfated species impractical.[19] In general, the associated dry eye syndrome makes it difficult to collect a sufficient amount of tear sample from patients to perform both glycan profile and structure elucidation. In this study, tear fluids were pooled into groups to obtain sufficient amounts to perform structure elucidation. Although the collection of saliva samples for analysis was easier, the saliva samples were similarly pooled for consistency.

Table 3. Neutral _O_-Glycans Isolated from Diseased Saliva by Positive Mode Nano LC CHIP Q-TOF MS[a]

peak ID	[M + Na]+	H	F	N	peak ID	[M + Na]+	H	F	N
1	1268.475	2	2	3	34	2160.792	5	2	5
2	1284.470	3	1	3	35	2217.839	3	6	4
3	1414.533	2	3	3	36	2224.797	7	3	3
4	1430.528	3	2	3	37	2233.834	4	5	4
5	1487.549	3	1	4	38	2249.829	5	4	4
6	1503.544	4		4	39	2274.860	3	5	5
7	1576.586	3	3	3	40	2281.818	7	2	4
8	1633.607	3	2	4	41	2290.855	4	4	5
9	1649.602	4	1	4	42	2306.850	5	3	5
10	1690.629	3	1	5	43	2363.872	5	2	6
11	1713.607	6	2	2	44	2370.855	7	4	3
12	1722.644	3	4	3	45	2379.892	4	6	4
13	1738.638	4	3	3	46	2395.887	5	5	4
14	1779.665	3	3	4	47	2427.876	7	3	4
15	1786.623	7		3	48	2436.913	4	5	5
16	1795.660	4	2	4	49	2443.871	8	2	4
17	1811.655	5	1	4	50	2452.908	5	4	5
18	1836.687	3	2	5	51	2468.903	6	3	5
19	1852.681	4	1	5	52	2493.935	4	4	6
20	1859.665	6	3	2	53	2516.913	7	5	3
21	1868.701	3	5	3	54	2541.944	5	6	4
22	1884.696	4	4	3	55	2582.971	4	6	5
23	1916.686	6	2	3	56	2589.929	8	3	4
24	1925.723	3	4	4	57	2598.966	5	5	5
25	1932.681	7	1	3	58	2671.982	6	3	6
26	1941.718	4	3	4	59	2678.966	8	5	3
27	1957.712	5	2	4	60	2735.987	8	4	4
28	1998.739	4	2	5	61	2745.024	5	6	5
29	2014.734	5	1	5	62	2761.019	6	5	5
30	2071.781	3	5	4	63	2818.040	6	4	6
31	2087.776	4	4	4	64	2907.077	6	6	5
32	2103.771	5	3	4	65	3028.103	8	6	4
33	2144.797	4	3	5					

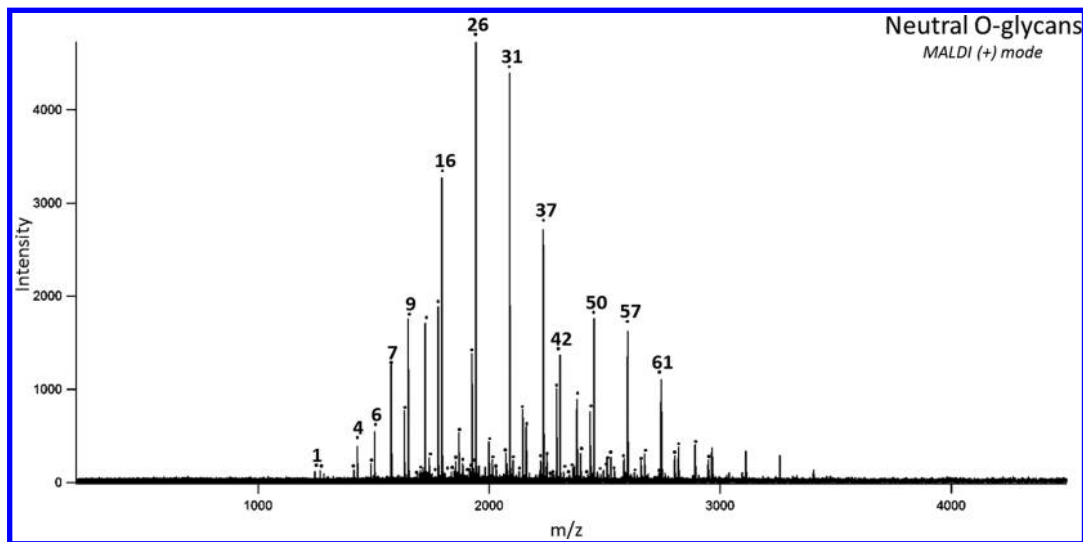[a]H = hexose, F = fucose, N = N-acetylhexosamine, SA = sialic acid, s = sulfate group.

Figure 2. Neutral _O_-glycans released from saliva of a patient with ocular rosacea obtained from positive mode MALDI FT-ICR MS. The label numbers correspond to specific glycan compositions listed in Table 3.
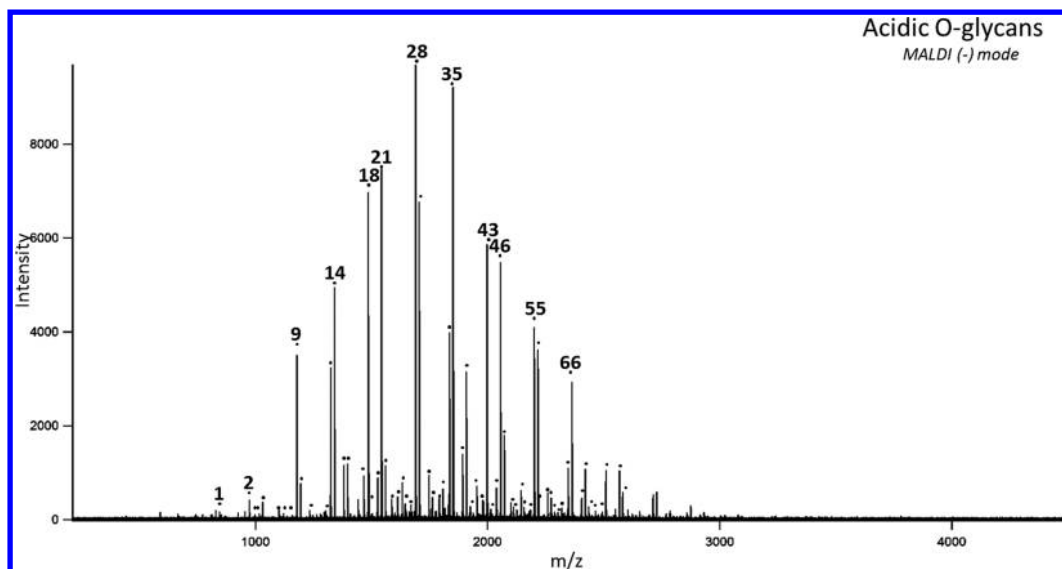
Figure 3. MALDI FT-ICR mass spectrum of *O*-glycans isolated from saliva of patient with ocular rosacea in negative mode. The label numbers correspond to specific glycan compositions listed in Table 4.

Saliva and tear samples were treated directly to release *O*-glycans using alkaline sodium borohydride, which is also the most commonly used method for releasing *O*-glycans.[40] A potential complication of releasing *O*-glycans from proteins is that *N*-glycans, when abundant, may also be released. There are two solutions for to deal with the issue. One is to remove the *N*-glycans first. However, removal of *N*-glycans with PNGase F is never complete, so *N*-glycan contamination can potentially never be eliminated. The other solution is to simply release the *O*-glcyans and use the MS characteristics of the peaks to distinguish one from the other. There are indications in the mass spectra to distinguish the two types. A common reaction for *N*-glycan under this release condition is the peeling reaction, which is the basic degradation of carbohydrates. These products, typically the loss of 60 and 90 mass units from integer monosaccharides values, are readily observed by MALDI FT-ICR MS.[40] The tandem MS of the glycans, described in greater detail below, also help differentiate between *N*- and *O*-glycans. *N*-Glycans yield distinct fragment ions such as those that correspond to the chitobiose (2HexNAc) core and the conserved *N*-glycan core (2HexNAc3Hex), which were not observed in any of the spectra.

Released *O*-glycans were purified and enriched using PGC before analysis by mass spectrometry. All glycan compositions were initially deduced from accurate masses. In order to minimize glycan suppression in the MS, *O*-glycans were fractionated according to their size and polarity using solid phase extraction with PGC. In this procedure, 20% AcN fractions yielded relatively smaller and neutral glycans while 40% AcN fraction yielded larger neutral and acidic glycans. In all, around 140 *O*-glycan compositions were obtained in both saliva and tear samples that we classify into four major types: (1) neutral, (2) sulfated (only), (3) sialylated (only), and (4) sulfated + sialylated species. Glycan belonging to groups 3 and 4 were further confirmed by LC−MS due to their low abundances as discussed in greater detail below.

O-Glycan Profile of Diseased Tear

Figure 1 shows the acidic *O*-glycan profile isolated from pooled diseased tear (*n* = 13) obtained by negative mode MALDI MS of the 40% fraction. As described previously, several of the samples contained insufficient amounts for analysis. For these samples, equal amounts were combined to yield a combined profile. MALDI MS profile of 20% fraction, which typically contained the neutral *O*-glycans, showed very few peaks (Supplementary Figure 1).The region between *m/z* 750 and 3500 of the 40% fraction yielded most of the signals in Figure 1. The spectra produced over 61 compositions that are tabulated in Table 1. Each compound is composed of various numbers of hexose (H), *N*-acetylhexosamine (N), fucose (F), sulfate (s), and sialic acid (SA). These glycans are described by the formula $[H_{2-7}, N_{2-7}, F_{0-5}, s_{0-2}, SA_{0-2}]$. Among this group, those that are sulfated (S > 0) make up the majority of the glycan species with the monosulfated (s = 1) being the most common. Species that are sialylated (only) and sulfated + sialylated were of relatively lower abundances in the diseased tear sample. For comparison, neutral *O*-glycans are relatively minor components in disease tear samples. The *O*-glycan MALDI MS profiles from all three fractions are shown in Supplementary Figure 1.

The mass profile of mixtures often leads to suppression of lowly abundant species. In order to characterize the less abundant species, the 20% and 40% fractions were combined and introduced directly to the nano flow LC CHIP-QTOF MS. Separation on PGC chip enabled detection as well as characterization of low abundant species. Table 2 lists at least 15 low abundant *O*-glycans that were found in diseased tear by this method but were not observed in the MALDI MS profile. Those glycans are either small neutral species or sialylated (only) and sulfated + sialylated acidic species.

O-Glycan Profile of Diseased Saliva

The rosacea diseased saliva is dominated by both neutral and anionic *O*-glycans. A representative MALDI MS spectrum of neutral *O*-glycan profile from diseased saliva is shown in Figure 2. Sixty-five neutral *O*-glycans isolated from diseased saliva with the formula $[H_{2-7}, N_{3-7}, \text{and } F_{0-6}]$ are listed in Table 3. The neutral *O*-glycans found in saliva are remarkably large and diverse. The majority of these glycans were uniquely fucosylated with some having as many as six fucoses. A recent report from this laboratory showed little variation in the neutral *O*-glycans between disease and control saliva.[40]

Acidic *O*-glycans, eluted with 40% AcN fractions, were also highly abundant in diseased saliva. In Figure 3, the dominant

Table 4. Acidic *O*-Glycans in Diseased Saliva Obtained by Negative Mode MALDI FT-ICR MS[a]

peak ID	[M − H]−	H	F	N	SA	s	peak ID	[M − H]−	H	F	N	SA	s
1	667.191	1		2		1	42	1980.672	3	2	4	1	1
2*	813.249	1	1	2		1	43	1997.677	4	3	4		1
3	829.241	2		2		1	44	2012.619	2		6	1	2
4*	870.266	1		3		1	45	2045.625	4		6		2
5	975.282	2	1	2		1	46	2054.700	4	2	5		1
6*	1016.308	1	1	3		1	47	2070.695	5	1	5		1
7*	1032.303	2		3		1	48	2086.687	6		5		1
8*	1121.357	2	2	2		1	49	2095.727	3	2	6		1
9	1178.379	2	1	3		1	50	2101.645	2	2	5	1	2
10	1194.374	3		3		1	51	2126.737	3	3	4	1	1
11*	1235.408	2		4		1	52	2141.744	7		2	2	
12*	1283.408	3	2	2		1	53	2183.749	3	2	5	1	1
13	1324.437	2	2	3		1	54	2184.772	3	4	5		1
14	1340.431	3	1	3		1	55	2200.758	4	3	5		1
15*	1381.462	2	1	4		1	56	2216.753	5	2	5		1
16	1397.459	3		4		1	57	2241.782	3	3	6		1
17	1470.498	2	3	3		1	58	2257.788	4	2	6		1
18	1486.484	3	2	3		1	59	2273.790	5	1	6		1
19*	1502.478	4	1	3		1	60	2289.798	4	5	4		1
20*	1527.520	2	2	4		1	61	2305.790	5	4	4		1
21	1543.506	3	1	4		1	62	2321.742	3	3	6		2
22	1559.512	4		4		1	63	2329.837	6	3	3	1	
23*	1584.556	2	1	5		1	64	2344.814	7		3	2	
24	1615.545	2	2	3	1	1	65	2346.824	4	4	5		1
25	1632.556	3	3	3		1	66	2362.811	5	3	5		1
26*	1648.547	4	2	3		1	67	2371.849	2	5	6		1
27*	1673.573	2	3	4		1	68	2403.844	4	3	6		1
28	1689.559	3	2	4		1	69	2435.829	6	1	6		1
29	1705.557	4	1	4		1	70	2449.765	2	1	6	2	2
30	1730.588	2	2	5		1	71	2465.759	3		6	2	2
31	1746.594	3	1	5		1	72	2549.899	4	4	6		1
32	1762.592	4		5		1	73	2611.821	3	1	6	2	2
33	1794.597	4	3	3		1	74	2622.918	5	2	7		1
34	1835.624	3	3	4		1	75	2636.935	7	2	3	2	
35	1851.611	4	2	4		1	76	2695.955	4	5	6		1
36	1867.625	5	1	4		1	77	2784.957	6	2	7		1
37	1892.656	3	2	5		1	78	2800.976	5	6	5		1
38	1908.648	4	1	5		1	79	2931.031	6	3	7		1
39	1924.660	3	5	3		1	80	2947.039	7	2	7		1
40	1938.609	4		3	2	1	81	3004.035	7	1	8		1
41	1965.658	4		6		1							

[a]Many are common to both tear and saliva. Those with asterisks represent compounds found only in saliva. H = hexose, F = fucose, N = *N*-acetylhexosamine, SA = sialic acid, s = sulfate group.

Table 5. Low Abundance *O*-Glycans Found in Diseased Saliva by Positive Mode Nano LC CHIP Q-TOF MS[a]

peak ID	[M]	H	F	N	SA	s
1	588.237	1		2		
2	734.295	1	1	2		
3	1201.346	2		2	2	1
4	1412.461	2	2	2		1
5	1558.519	2	1	2	2	1

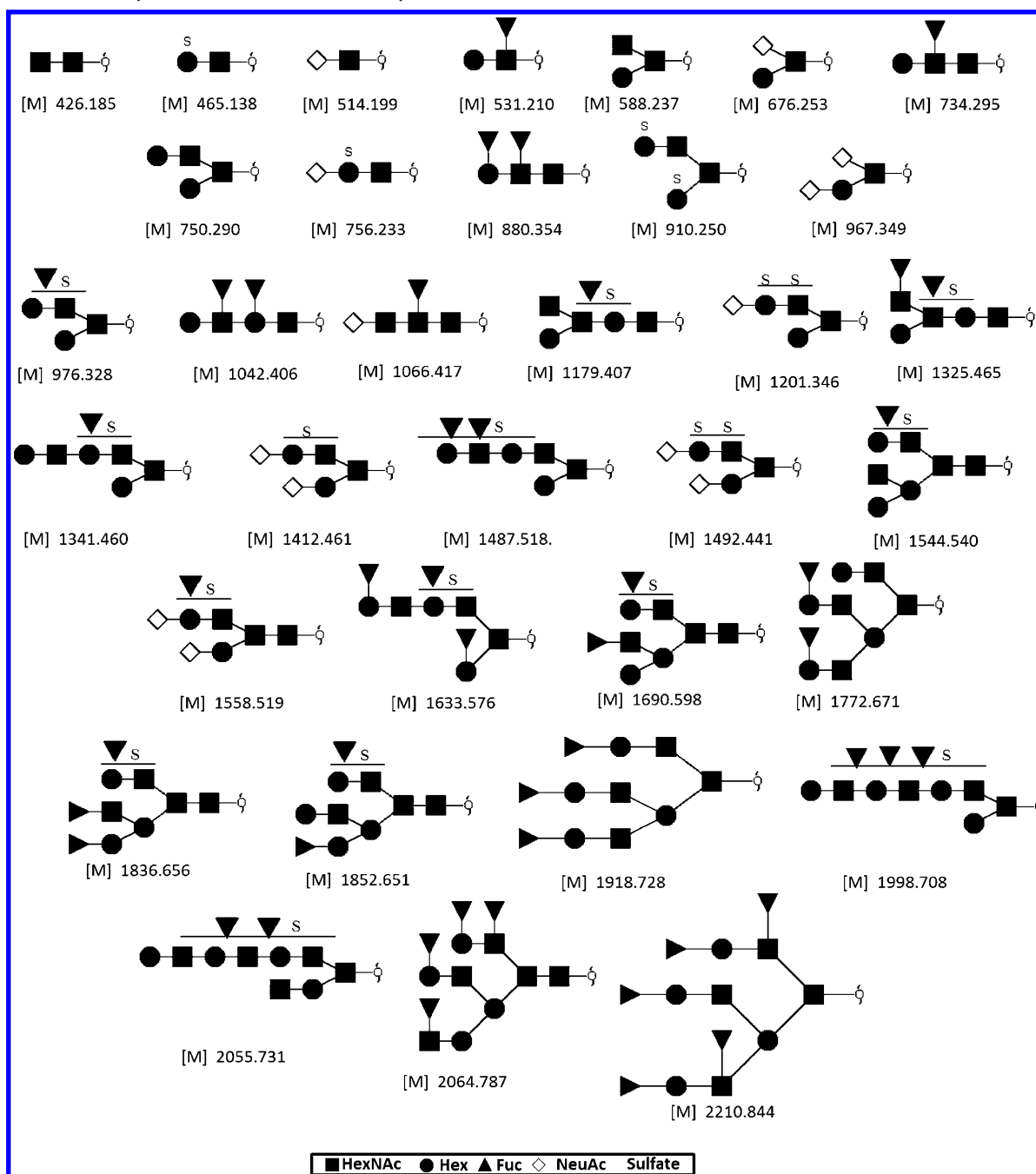[a]H = hexose, F = fucose, N = *N*-acetylhexosamine, SA = sialic acid, s = sulfate group.

signals correspond to acidic species with the majority being sulfated as was observed in diseased saliva. The series of acidic *O*-glycans found in saliva are listed in Table 4. The group consisting of *m/z* 1689.56, 1851.61, 1543.51, 1340.44, 1486.49 corresponds to the top five most abundant sulfated *O*-glycans with compositions corresponding to $[H_3N_4F_2s_1]$, $[H_4:N_4:F_2:s_1]$, $[H_3:N_4:F_1:s_1]$, $[H_3:N_3:F_1:s_1]$, $[H_3:N_3:F_2:s_1]$, respectively. The same acidic species were found in controls but were significantly decreased.[40] However, the number of glycans that were found in diseased saliva was higher than that of diseased tear samples.

As with tears, low abundant species in saliva were also observed and characterized by nano LC CHIP Q-TOF MS. These species comprise mainly neutral and sulfated + sialylated species. Table 5 gives the compositions of these species in diseased saliva. The compositions were further confirmed with CID (tandem MS).

Structural Elucidation by Tandem MS

To obtain structural information, tandem MS using collision-induced dissociation CID and infrared multiphoton dissociation (IRMPD) in the FT ICR and CID in the Q-TOF were used.

Chart 1. Partial *O*-Glycan Structures Elucidated by CID Tandem MS[a]

[M] 426.185   [M] 465.138   [M] 514.199   [M] 531.210   [M] 588.237   [M] 676.253   [M] 734.295

[M] 750.290   [M] 756.233   [M] 880.354   [M] 910.250   [M] 967.349

[M] 976.328   [M] 1042.406   [M] 1066.417   [M] 1179.407   [M] 1201.346   [M] 1325.465

[M] 1341.460   [M] 1412.461   [M] 1487.518.   [M] 1492.441   [M] 1544.540

[M] 1558.519   [M] 1633.576   [M] 1690.598   [M] 1772.671

[M] 1836.656   [M] 1852.651   [M] 1918.728   [M] 1998.708

[M] 2055.731   [M] 2064.787   [M] 2210.844

■ HexNAc ● Hex ▲ Fuc ◇ NeuAc — Sulfate

[a] circle = hexose, square = *N*-acetyl hexoseamine, triangle = fucose, S = sulfate (SO$_3$H).

Shown in Chart 1 is a summary of the partial structures deduced by tandem MS as described below for neutral, sulfated, sialylated, and sulfated + sialylated species. These compounds were selected because they were present in both tear and saliva. Tandem MS was ideal for obtaining structural information of sulfated species in the MALDI FT-ICR/MS. For compounds that were weakly abundant such as the sulfated species, tandem MS experiments in the QTOF were performed.

Neutral *O*-Glycans. Structural elucidation of a representative neutral glycan using CID in the MALDI FTICR is illustrated in Figure 4. This species is relatively large for an *O*-glycan with the composition [H$_4$N$_3$F$_4$N$_1$-ol + Na] obtained from accurate mass. Tandem MS provides general structural features as well as the composition. It also produces a number of fragmentation pathways; following these pathways yields information to aid in elucidating the structures. In Figure 4, the MS/MS spectrum shows 4 representative pathways. For each pathway, there exists an initial loss of one [F] to yield *m/z* 1941.104. There are no other residues lost from the molecular ion, suggesting that all antennae are capped with [F]. The first pathway (1) contains the loss of [F] followed by the loss of [H + N] (1576.179-label in spectra) indicating the presence of lactose amine. Additionally, sequential losses of 3 fucoses after (1576.179) yielded *m/z* 1138.203, followed by the loss of a second lactosamine. The pathway 1 ends up with *m/z* 773.184, which corresponds to [H$_2$N$_1$N$_1$-ol + Na]. This pathway provides the following
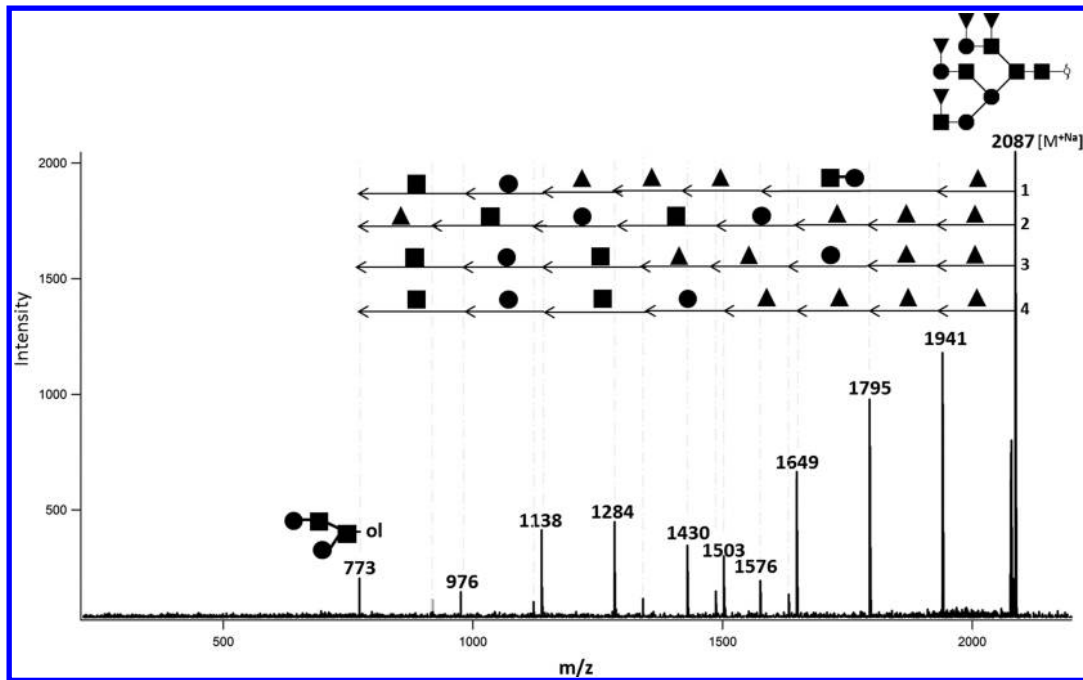
Figure 4. Representative CID tandem mass spectra used for the structure elucidation of neutral *O*-glycans isolated from saliva. circle = hexose, square = *N*-acetyl hexoseamine, triangle = fucose, S = sulfate (SO₃H).
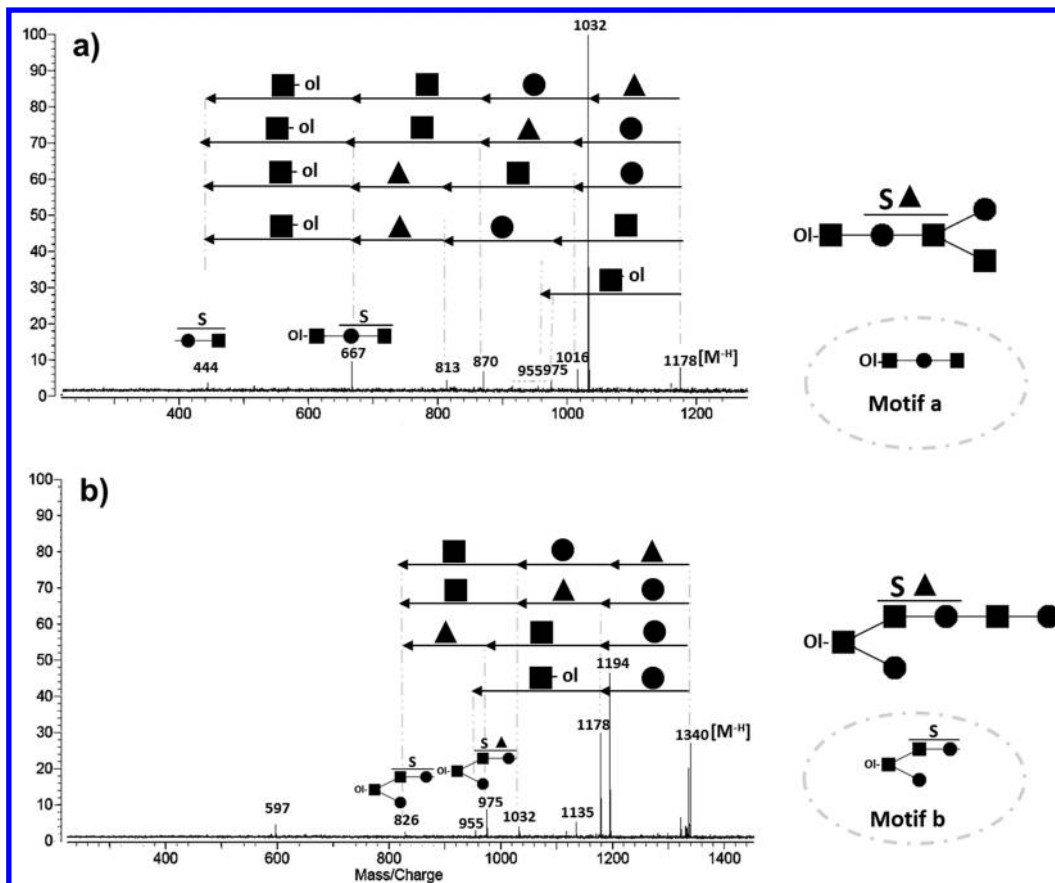

Figure 5. Representative MALDI FT ICR MS CID spectra of pooled patient saliva: (a) CID fingerprinting of *core1* mucin-type *O*-glycan including motif **a**. (b) Fragmentation pattern of *core 2* mucin-type *O*-glycan composed of motif **b**. circle = hexose, square = *N*-acetyl hexoseamine, ▲ = fucose, S = sulfate (SO₃H).

information: (i) the glycan composition is confirmed by sequential residue losses, (ii) the glycan has more than one lactosamine group, and (iii) the four fucoses are on terminal positions. Pathway 3 shows the loss of [F] followed by [H],
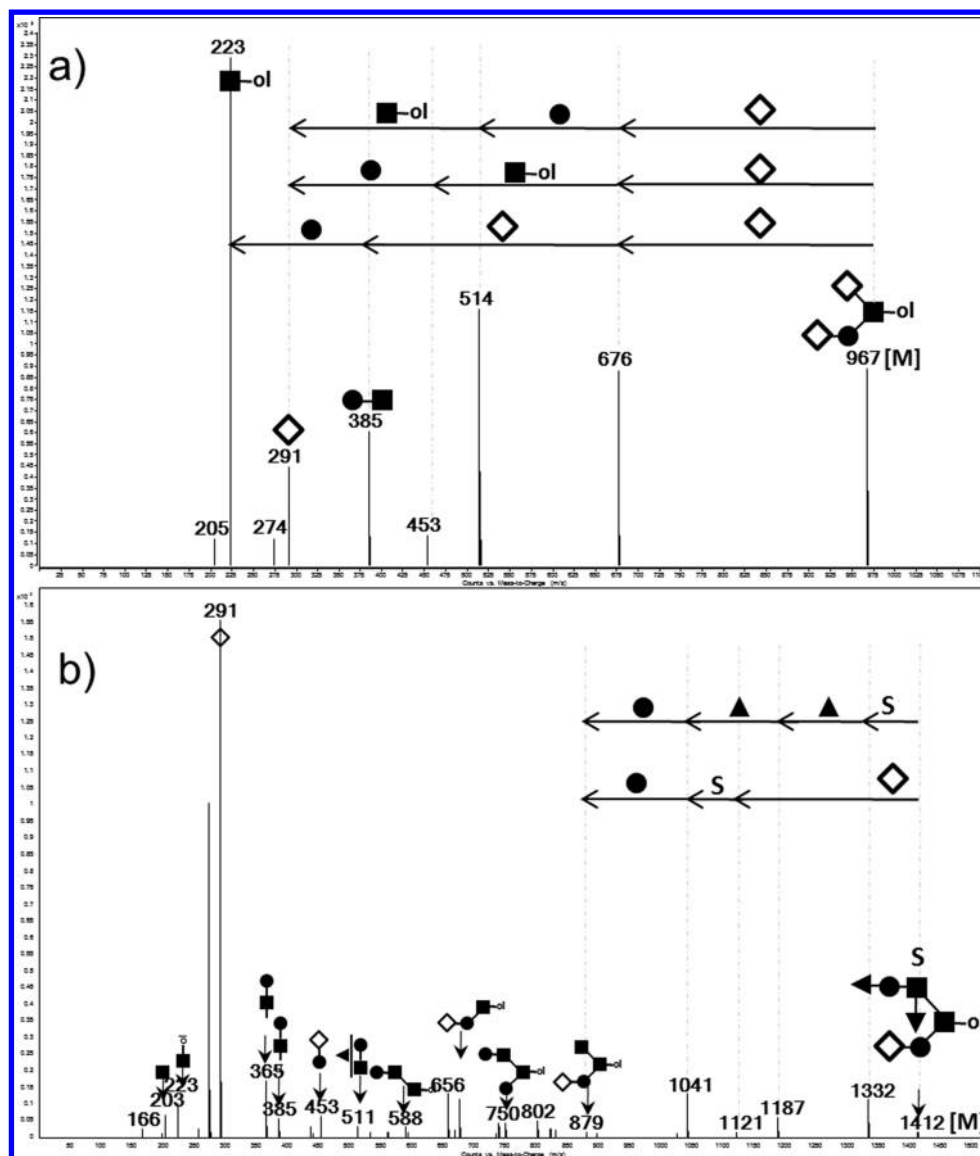
Figure 6. Tandem mass spectra of (a) disialylated and (b) sulfated-sialylated *O*-glycans isolated from individual patient tear obtained by chip-based nano-LC Q-TOF. circle = hexose, square = *N*-acetyl hexoseamine, triangle = fucose, S = sulfate (SO$_3$H).

consistent with a terminal [F + H]. There are no losses of [N] immediately after the loss of [F] in any of the pathways. Thus, [N] is not at a terminal position further suggesting that all terminal fucoses are attached to hexoses. The structure that best fits this fragmentation pattern is given in Figure 4 (inset). This approach was used to elucidate all structures listed in Chart 1. Because no chromatographic separation was performed, these compositions may be due to several isomers. However, the tandem MS are consistent with the connectivity so that the isomers may be primarily due to variations in linkages.

Sulfated *O*-Glycans. We confirm the presence of sulfated groups in the tandem MS. Representative tandem spectra of MALDI FT ICR MS of *core 1*- and *core 2*-type sulfated *O*-glycans are shown in Figure 5. The tandem MS of the ion at *m/z* 1178.378 consisting of [H$_2$:N$_2$:F$_1$:s$_1$:N-ol$_1$] was shown in Figure 5a. Four different pathways were observed in the tandem MS spectra. [H], [F], [N], and reducing end losses from molecular ion indicate that those four residues should be placed at the terminal positions. *Core 2* structures are readily differentiated from *core 1* because the former is branched at the reducing

terminus, while the latter maintains a linear structure. *Core 2* structures cannot therefore lose the reducing end, whereas core 1 structures can. The loss of the reducing end alditol (-ol) was therefore used as a unique indicator for distinguishing *core 1* from the *core 2* type structures. The presence of [N-ol] loss and motif a [H$_1$:N$_1$:N-ol$_1$ − H] demonstrated the presence of a *core 1* mucin-type *O*-glycan. On the other hand, 1340.430 corresponds to [H$_3$:N$_2$:F$_1$:s$_1$:N-ol$_1$]. The composition is confirmed by CID as shown in Figure 5b. The losses of [F] (*m/z* 1194), [H] (*m/z* 1178, and [N] (*m/z* 975) from the molecular ion at *m/z* 1178 indicate that three residues (H, N, and F) are present as nonreducing termini. The latter two ions subsequently lose a [H] and [N], respectively, to yield *m/z* 975. In parallel, the fragment ion *m/z* 829 [H$_2$:N$_1$:s$_1$:N-ol$_1$ − H] was obtained from the loss of [F] in 975 *m/z*.From the tandem mass spectra, it can be readily deduced that the [N] residue loss is only possible after the loss of the [H] residue. The fragmentation pattern suggests that the reducing terminus, [N-ol], links to both [H] and [N], which indicates *core 2*-type *O*-glycans. The presence of motif b *m/z* 829 [H$_2$:N$_1$:s$_1$:N-ol$_1$ − H] corresponds to *core 2* mucin-type *O*-

glycan. The majority of sulfated glycans are *core 1*- and *core 2*-type *O*-glycans. In all the sulfated structures observed, tandem MS data suggest that the sulfate group is located in an internal position bound to either [H] or [N]. While tandem MS cannot precisely determine the position of the sulfate group, it has been previously reported that sulfate groups in mucins human are attached to C-3, C-4, or C-6 of a galactose or C-6 of *N*-acetylglucosamine.[41] It should be noted that in these tandem MS spectra, losses of the sulfate groups are not observed.

Sialylated *O*-Glycans. Oligosaccharides containing only sialic acid or both sulfate and sialic acid, simultaneously, could not be readily observed in the MALDI MS profile described above because of their low abundances. To observe these structures, it was necessary to separate the compounds using chromatography. Figure 6a represents a tandem MS of a sialylated *O*-glycan obtained from nano LC Q-TOF MS/MS. This small compound distributes the sialic acid between the two constituent of a *core 1* motif. The sialic acid loss from the precursor ion (m/z 676.270) shows the sialic acid at the terminal position. Furthermore, the loss of the reducing end (N-ol) yields m/z 453.190, which corresponds to [H + SA]. The same glycan structure that has been previously reported from several sources including saliva,[42] endocrine gland,[43] and intestine colon mucosa.[44]

An example of a sialylated and sulfated *O*-glycan fragmentation pattern is shown in Figure 6b. There are two main fragmentation pathways that suggest the presence of sulfation, sialylation, and fucosylation. The initial losses of sulfate group and sialic acid suggest that these two residues are at the terminal position. The spectrum contains a number of small fragment ions that yield structural information as annotated in Figure 6b. The proposed structure is provided in the figure based on the fragment ions observed. This structure corresponds to that previously reported and isolated from respiratory mucins.[27]

CONCLUSION

The simultaneous analysis of saliva and tear fluid shows a correlation between the two fluids interms of glycan content as we previously discussed in detail.[40] The structure of the most abundant components, found in both tear and saliva, are now elucidated and presented in Chart 1 as determined by tandem MS. They range in size from small di- and trisaccharides, typical for *O*-glycans, but some are quite large for *O*-glycans, consisting of over 10 residues.

Tear and saliva from patients with ocular rosacea are rich in sulfated glycans. Sulfated oligosaccharides are the most abundant anionic component, with a single sulfated group and little or no di- and trisulfated species detected. Because both tear and saliva are rich in mucins, the glycans presented here are likely released from mucin proteins. The increase in sulfation may have major consequences in the tear and saliva fluids. They alter the physical properties of the mucins relative to neutral glycans, making them more anionic and in turn changing their interactions with epithelial cells.

The differences in mucin glycosylation accompanying rosacea may affect the microbiome in the eyes and in the mouth. It has been previously shown that glycosylation can mediate specific binding between host cells and the microbiome.[45] Further studies indicate that mucin sulfation and sialylation further modulate bacterial interactions.[45] Both sulfate (sulfomucins) and sialic acid containing mucins (sialomucins) give the mucins their overall negative charge, which contribute extra protection from bacterial degradation due to their resistance to most bacterial

mucin-degrading enzymes.[46] From this perspective, changes in the abundances of acidic *O*-glycans in the tear and saliva of rosacea patient may signal a potential change in the interaction between the host and its microbiome. This situation could further lead to a change in the microbiome perhaps favoring specific groups of bacteria. We therefore encourage future studies that examine changes in the microbiomes of mouth and eye of dry eye diseases such as rosacea.

AUTHOR INFORMATION

Corresponding Author

*E-mail: lebrilla@chem.ucdavis.edu.

Notes

The authors declare no competing financial interest.

REFERENCES

(1) Taniguchi, N. Toward cancer biomarker discovery using the glycomics approach. *Proteomics* **2008**, *8* (16), 3205−3208.

(2) Chen, C. C.; Engelborghs, S.; Dewaele, S.; Le Bastard, N.; Martin, J. J.; Vanhooren, V.; Libert, C.; De Deyn, P. P. Altered serum glycomics in Alzheimer Disease: A potential blood biomarker? *Rejuvenation Res.* **2010**, *13* (4), 439−444.

(3) Leiserowitz, G. S.; Lebrilla, C.; Miyamoto, S.; An, H. J.; Duong, H.; Kirmiz, C.; Ll, B.; Liu, H.; Lam, K. S. Glycomics analysis of serum: a potential new biomarker for ovarian cancer? *Int. J. Gynecol. Cancer* **2008**, *18* (3), 470−475.

(4) Narimatsu, H.; Kameyama, A.; Hirabayashi, J. Novel strategies for glycomics biomarker research. *Mol. Cell. Proteomics* **2006**, *5* (10), S330−S330.

(5) An, H. J.; Kronewitter, S. R.; de Leoz, M. L. A.; Lebrilla, C. B. Glycomics and disease markers. *Curr. Opin. Chem. Biol.* **2009**, *13* (5−6), 601−607.

(6) Lebrilla, C. B.; An, H. J. The prospects of glycan biomarkers for the diagnosis of diseases. *Mol. Biosyst.* **2009**, *5* (1), 17−20.

(7) Lebrilla, C. B.; Mahal, L. K. Post-translation modifications. *Curr. Opin. Chem. Biol.* **2009**, *13* (4), 373−374.

(8) An, H. J.; Froehlich, J. W.; Lebrilla, C. B. Determination of glycosylation sites and site-specific heterogeneity in glycoproteins. *Curr. Opin. Chem. Biol.* **2009**, *13* (4), 421−426.

(9) Apweiler, R.; Hermjakob, H.; Sharon, N. On the frequency of protein glycosylation, as deduced from analysis of the SWISS-PROT database. *Biochim. Biophys. Acta, Gen. Subj.* **1999**, *1473* (1), 4−8.

(10) Lebrilla, C. B.; Xie, Y. M. Determination of oligosaccharide diversity by mass spectrometry. *Abstr. Pap. Am. Chem. Soc.* **2002**, *224*, U321−U321.

(11) Royle, L.; Mattu, T. S.; Hart, E.; Langridge, J. I.; Merry, A. H.; Murphy, N.; Harvey, D. J.; Dwek, R. A.; Rudd, P. M. An analytical and structural database provides a strategy for Sequencing *O*-glycans from microgram quantities of glycoproteins. *Anal. Biochem.* **2002**, *304* (1), 70−90.

(12) Chu, C. S.; Ninonuevo, M. R.; Clowers, B. H.; Perkins, P. D.; An, H. J.; Yin, H. F.; Killeen, K.; Miyamoto, S.; Grimm, R.; Lebrilla, C. B.

Profile of native N-linked glycan structures from human serum using high performance liquid chromatography on a microfluidic chip and time-of-flight mass spectrometry. *Proteomics* **2009**, *9* (7), 1939−1951.

(13) Xie, Y.; Schubothe, K. M.; Hedrick, J. L.; Lebrilla, C. B. Structural analysis of sulfated O-linked oligosaccharides in glycoproteins by mass spectrometry. *Mol. Biol. Cell* **2002**, *13*, 109a−109a.

(14) Zhang, J. H.; Lindsay, L. L.; Hedrick, J. L.; Lebrilla, C. B. Strategy for profiling and structure elucidation of mucin-type oligosaccharides by mass spectrometry. *Anal. Chem.* **2004**, *76* (20), 5990−6001.

(15) Thomsson, K. A.; Schulz, B.; Packer, N. H.; Karlsson, N. G. Human salivary mucins: MG2 (MUC7) glycosylation is consistent, whereas MGI (MUC5B) glycosylation varies extensively between healthy individuals. *Glycobiology* **2005**, *15* (11), 1216−1216.

(16) Wu, A. M.; Csako, G.; Herp, A. Structure, biosynthesis, and function of salivary mucins. *Mol. Cell. Biochem.* **1994**, *137* (1), 39−55.

(17) Xia, B. Y.; Royall, J. A.; Damera, G.; Sachdev, G. P.; Cummings, R. D. Altered O-glycosylation and sulfation of airway mucins associated with cystic fibrosis. *Glycobiology* **2005**, *15* (8), 747−775.

(18) Sumiyoshi, M.; Ricciuto, J.; Tisdale, A.; Gipson, I. K.; Mantelli, F.; Argueso, P. Antiadhesive character of mucin O-glycans at the apical surface of corneal epithelial cells. *Invest. Ophthalmol. Visual Sci.* **2008**, *49* (1), 197−203.

(19) An, H. J.; Ninonuevo, M.; Aguilan, J.; Liu, H.; Lebrilla, C. B.; Alvarenga, L. S.; Mannis, M. J. Glycomics analyses of tear fluid for the diagnostic detection of ocular rosacea. *J. Proteome Res.* **2005**, *4* (6), 1981−1987.

(20) Loguidice, J. M.; Wieruszeski, J. M.; Lemoine, J.; Verbert, A.; Roussel, P.; Lamblin, G. Sialylation and Sulfation of the carbohydrate chains in respiratory mucins from a patient with cystic-fibrosis. *J. Biol. Chem.* **1994**, *269* (29), 18794−18813.

(21) Seipert, R. R.; Barboza, M.; Ninonuevo, M. R.; LoCascio, R. G.; Mills, D. A.; Freeman, S. L.; German, J. B.; Lebrilla, C. B. Analysis and quantitation of fructooligosaccharides using matrix-assisted laser desorption/ionization Fourier transform ion cyclotron resonance mass spectrometry. *Anal. Chem.* **2008**, *80* (1), 159−165.

(22) Furr, A. E.; Ranganathan, S.; Finn, O. J. Aberrant expression of MUC1Mucin in pediatric inflammatory bowel disease. *Pediatr. Dev. Pathol.* **2010**, *13* (1), 24−31.

(23) Kirkham, S.; Kolsum, U.; Rousseau, K.; Singh, D.; Vestbo, J.; Thornton, D. MUC5B is the major mucin in the gel phase of sputum in chronic obstructive pulmonary disease. *Am. J. Resp. Crit. Care* **2008**, *178* (10), 1033−1039.

(24) Mattar, A. F.; Coran, A. G.; Teitelbaum, D. H. MUC-2 mucin production in Hirschsprung's disease: Possible association with enterocolitis development. *J. Pediatr. Surg.* **2003**, *38* (3), 417−421.

(25) Smith, R. F.; Stern, B. H.; Smith, A. A. Mucin immunohistochemistry in the diagnosis and mapping of extramammary Paget's disease. *J. Cell. Mol. Med.* **2008**, *12* (5A), 1605−1610.

(26) Guzman-Aranguez, A.; Mantelli, F.; Argueso, P. Mucin-type O-glycans in tears of normal subjects and patients with non-Sjogren's dry eye. *Invest. Ophthalmol. Visual Sci.* **2009**, *50* (10), 4581−4587.

(27) Lamblin, G.; Degroote, S.; Perini, J. M.; Delmotte, P.; Scharfman, A. E.; Davril, M.; Lo-Guidice, J. M.; Houdret, N.; Dumur, V.; Klein, A.; Roussel, P. Human airway mucin glycosylation: A combinatory of carbohydrate determinants which vary in cystic fibrosis. *Glycoconjugate J.* **2001**, *18* (9), 661−684.

(28) Guzman-Aranguez, A.; Argueso, P. Structure and biological roles of mucin-type O-glycans at the ocular surface. *Ocul. Surf.* **2010**, *8* (1), 8−17.

(29) Geng, Y.; Marshall, J. R.; King, M. R. Glycomechanics of the metastatic cascade: tumor cell-endothelial cell interactions in the circulation. *Ann. Biomed. Eng.* **2012**, *40* (4), 790−805.

(30) Holmen, J. M.; Karlsson, H.; Thomsson, K. A.; Sjvall, H.; Hansson, G. C. Mapping of mucin O-glycosylation patterns in human colonic biopsies. *Glycobiology* **2004**, *14* (11), 1164−1164.

(31) Fukuda, M. Roles of mucin-type O-glycans in cell adhesion. *Biochim. Biophys. Acta, Gen. Subj.* **2002**, *1573* (3), 394−405.

(32) Zhang, J. H.; Schubothe, K.; Li, B. S.; Russell, S.; Lebrilla, C. B. Infrared multiphoton dissociation of O-linked mucin-type oligosaccharides. *Anal. Chem.* **2005**, *77* (1), 208−214.

(33) Veerman, E. C. I.; Bank, C. M. C.; Namavar, F.; Appelmelk, B. J.; Bolscher, J. G. M.; Amerongen, A. V. N. Sulfated glycans on oral mucin as receptors for Helicobacter pylori. *Glycobiology* **1997**, *7* (6), 737−743.

(34) Namavar, F.; Sparrius, M.; Veerman, E. C. I.; Appelmelk, B. J.; Vandenbroucke-Grauls, C. M. J. E. Neutrophil-activating protein mediates adhesion of Helicobacter pylori to sulfated carbohydrates on high-molecular-weight salivary mucin. *Infect. Immun.* **1998**, *66* (2), 444−447.

(35) Namavar, F.; Sparrius, M.; Veerman, E. C. I.; Appelmelk, B. J.; VandenbrouckeGrauls, C. M. J. E. Identification of a Helicobacter pylori adhesin recognizing sulfated oligosaccharide. *Gut* **1997**, *41*, A108−A108.

(36) Kawashima, H. Roles of sulfated Glycans in lymphocyte homing. *Biol. Pharm. Bull.* **2006**, *29* (12), 2343−2349.

(37) Gudmundsen, K. J.; Odonnell, B. F.; Powell, F. C. Schirmer testing for dry eyes in patients with rosacea. *J. Am. Acad. Dermatol.* **1992**, *26* (2), 211−214.

(38) Lemp, M. A.; Mahmood, M. A.; Weiler, H. H. Association of rosacea and keratoconjunctivitis sicca. *Arch Ophthalmol. (Chicago, IL, U.S.)* **1984**, *102* (4), 556−557.

(39) Tanzi, E. L.; Weinberg, J. M. The ocular manifestations of rosacea. *Cutis* **2001**, *68* (2), 112−114.

(40) Vieira, A. C.; An, H. J.; Ozcan, S.; Kim, J. H.; Lebrilla, C. B.; Mannis, M. J. Glycomic analysis of tear and saliva in ocular rosacea patients: the search for a biomarker. *Ocul. Surf.* **2012**, *10* (3), 184−92.

(41) Mawhinney, T. P.; Adelstein, E.; Gayer, D. A.; Landrum, D. C.; Barbero, G. J. Structural-analysis of monosulfated side-chain oligosaccharides isolated from human tracheobronchial mucous glycoproteins. *Carbohydr. Res.* **1992**, *223*, 187−207.

(42) Strecker, G.; Wieruszeski, J. M.; Martel, C.; Montreuil, J. Determination of the structure of sulfated tetrasaccharides and pentasaccharides obtained by alkaline borohydride degradation of hen ovomucin - a fast atom bombardment-mass spectrometric and H-1-NMR spectroscopic study. *Glycoconjugate J.* **1987**, *4* (4), 329−337.

(43) Edge, A. S. B.; Spiro, R. G. Structure of the O-linked oligosaccharides from a major thyroid cell surface glycoprotein. *Arch. Biochem. Biophys.* **1997**, *343* (1), 73−80.

(44) Capon, C.; Laboisse, C. L.; Wieruszeski, J. M.; Maoret, J. J.; Augeron, C.; Fournet, B. Oligosaccharide structures of mucins secreted by the human colonic cancer cell line CL.16E. *J. Biol. Chem.* **1992**, *267* (27), 19248−57.

(45) Berry, M.; Harris, A.; Lumb, R.; Powell, K. Commensal ocular bacteria degrade mucins. *Br. J. Ophthalmol.* **2002**, *86* (12), 1412−1416.

(46) Derrien, M.; van Passel, M. W. J.; van de Bovenkamp, J. H. B.; Schipper, R.; de Vos, W.; Dekker, J. Mucin-bacterial interactions in the human oral cavity and digestive tract. *Gut Microbes* **2010**, *1* (4), 254−268.